

A Kazal prolyl endopeptidase inhibitor isolated from the skin of *Phyllomedusa sauvagii*

Leopoldo G. Gebhard^{1,5}, Federico U. Carrizo¹, Ana L. Stern¹, Noelia I. Burgardt¹, Julián Faivovich^{2,3}, Esteban Lavilla^{4,5} and Mario R. Ermácora^{1,5}

¹Departamento de Ciencia y Tecnología, Universidad Nacional de Quilmes, Argentina; ²American Museum of Natural History, New York, USA; ³División Herpetología, Museo Argentino de Ciencias Naturales, Buenos Aires, Argentina; ⁴Instituto de Herpetología Miguel Lillo, Tucumán, Argentina; ⁵Consejo Nacional de Investigaciones Científicas y Técnicas, Argentina

Searching for bioactive peptides, we analyzed acidic extracts of *Phyllomedusa sauvagii* skin and found two new proteins, PSKP-1 and PSKP-2, of 6.7 and 6.6 kDa, respectively, which, by sequence homology, belong to the Kazal family of serine protease inhibitors. PSKP-1 and PSKP-2 exhibit the unprecedented feature of having proline at P₁ and P₂ positions. A gene encoding PSKP-1 was synthesized and expressed in *Escherichia coli*. Recombinant PSKP-1 was purified from inclusion bodies, oxidatively refolded to the native state, and characterized by chemical, hydrodynamic and optical studies. PSKP-1 shows inhibitory activity against a serum prolyl endopeptidase, but is unable to inhibit trypsin,

chymotrypsin, V8 protease, or proteinase K. In addition, PSKP-1 can be rendered active against trypsin by active-site site-specific mutagenesis, has bactericidal activity, and induces agglutination of red cells at micromolar concentrations. PSKP-1 might protect *P. sauvagii* teguments from microbial invasion, by acting as an inhibitor of an as-yet unidentified prolyl endopeptidase or directly as a microbicidal compound.

Keywords: Kazal; protease inhibitor; anurans; *Phyllomedusa sauvagii*; antimicrobial peptide.

To date, several hundred bioactive compounds have been isolated from the skin of amphibians, and this number is growing rapidly. The list includes biogenic amines, alkaloids, sterols and peptides with a plethora of biological effects (i.e. cytotoxic, bactericidal, fungicidal, lytic, neuro-mimetic, anaesthetic and pheromonal) [1–8]. Many peptides, grouped in several structural classes, have been isolated from anurans of the hyliid subfamily *Phyllomedusinae*: tachykinins, bradykinins, caeruleins, bombesins, sauvagine, opioid peptides (dermorphins and deltorphins), antimicrobial peptides (dermasseptins and adenoregulin), and tryptophylins [7,9–12]. Interest in these natural products stems from the need for lead compounds in drug

discovery and from their contribution to our understanding of biodiversity at a molecular level.

Recently, protease inhibitors have been added to the above list. The first, named Bombina skin trypsin inhibitor (BSTI), was isolated from *Bombina orientalis* and pertains to a family of protease inhibitors discovered in nematodes and honeybees [13,14]. A closely related peptide was purified from the Chinese red-belly toad *B. maxima* [15]. Later, a typical member of the Kunitz family, similar to bovine pancreatic trypsin inhibitor, was found in the skin of the tomato frog *Dyscophus guineti* [16]. Also, in *Rana areolata*, the following were identified: a peptide that inhibited porcine trypsin and possessed the 10-cysteine-residue motif characteristic of BSTI; a protein with the whey acidic protein motif (also called the ‘four-disulfide core’ motif), characteristic of skin-derived anti-leukoproteases; and a secretory leukocyte protease inhibitor [17]. The biological function of these inhibitors is, to date, unknown. However, they may control propeptide processing during the production of other bioactive peptides, and/or have inhibitory effects on proteases from microbes that attempt to invade teguments [13,16].

In this study, we show that the skin of *Phyllomedusa sauvagii* contains two novel Kazal proteins homologous to pancreatic secretory trypsin inhibitor (PSTI). We have named these cysteine-rich highly basic variants PSKP-1 and PSKP-2 (*P. sauvagii* Kazal proteins 1 and 2). The putative active site of PSKP-1 and PSKP-2 exhibits the unprecedented feature of having proline at P₁ and P₂ positions. PSKP-1, overexpressed as a recombinant protein in *Escherichia coli*, is naturally inactive against trypsin-like serine proteases, but it could be converted into a potent trypsin inhibitor by

Correspondence to M. R. Ermácora, Departamento de Ciencia y Tecnología, Universidad Nacional de Quilmes, Roque Sáenz Peña 180 (B1876BXD) Bernal, Argentina. Fax: + 54 114 365 7132, Tel.: + 54 114 365 7100, E-mail: ermacora@unq.edu.ar

Abbreviations: BSTI, *Bombina* skin trypsin inhibitor; EC₅₀, effective concentration that causes 50% of the observed effect; IC₅₀, concentration that causes 50% inhibition; PSKP, *P. sauvagii* Kazal protein; PSKP-1^K, PSKP-1 variant with L, P, G and K at position P₆, P₅, P₄, and P₁, respectively; PSTI, pancreatic secretory trypsin inhibitor; SEC, size exclusion chromatography; Z-Arg-pNA, *N*-benzyloxycarbonyl-arginyl-*p*-nitroanilide; Z-Gly-Pro-2-NNap, *N*-benzyloxycarbonyl-glycyl-prolyl-2-naphthylamide.

Note: The protein sequence data reported in this paper will appear in the SWISS-PROT and TrEMBL knowledge base under the accession numbers P83578 and P83579.

(Received 19 January 2004, revised 23 March 2004, accepted 30 March 2004)

active-site site-specific mutagenesis, indicating that PSKP-1 and PSTI have similar 3D structures.

Most interestingly, at submicromolar concentrations, PSKP-1 was found to possess *in vitro* inhibitory activity towards a prolyl endopeptidase from blood serum. Moreover, like aprotinin, lysozyme, lactoferrin, and other polycations [18,19], PSKP-1 displays bactericidal activity at micromolar concentrations and induces agglutination of red cells and bacteria. Thus, PSKP-1 might act *in vivo* as a prolyl endopeptidase inhibitor and/or have a role in mucosal defense against microbes by direct interaction with their membranes.

Materials and methods

Materials

All chemicals were of the purest analytical grade available. Proteases, aprotinin, lysozyme, and α -casein were from Sigma-Aldrich. Z-Arg-pNA (*N*-benzyloxycarbonyl-arginyl-*p*-nitroanilide) and Z-Gly-Pro-2-NNap (*N*-benzyloxycarbonyl-glycyl-prolyl-2-naphthylamide) were from Bachem Bioscience Inc. (King of Prussia, PA, USA). Acetyl cellulose dialysis membranes (1 kDa cut-off) were Spectra/Por from Spectrum Medical Industries Inc. (Houston, TX, USA).

General methods

Peptides were sequenced using an Applied Biosystems 470A instrument (LANAIS-CONICET Facility; Buenos Aires, Argentina). Electrospray mass analysis was performed on a VG Biotech/Fisons (Altrincham, UK) triple-quadrupole spectrometer. SDS/PAGE was performed as described previously [20]. Two chromatography instruments were utilized: the first was a Waters 2690 Alliance Separation Module (Waters, Milford, MA, USA) equipped with Waters 2487 Dual λ absorbance detector, and the second was an FPLC system (Pharmacia, Uppsala, Sweden). Free thiols were determined by using Ellman's procedure [21]. DNA was custom-sequenced at the University of Chicago (Chicago, IL, USA).

Preparation of the frog skin extract

The single *P. savagii* specimen used in this work was captured in the region of El Cadillal (Tucumán, Argentina). Care and experiments followed the Canadian Council on Animal Care recommendations. The frog was pithed and its skin was immediately removed, cut into small pieces, and stored for several weeks at 4 °C in 60 mL of 20% (v/v) acetic acid before processing. Then, the extract was filtered, dialyzed against distilled water, and lyophilized.

Protein purification and chemical characterization

The lyophilized extract was dissolved (at a concentration of 20 mg·mL⁻¹) in buffer A (20 mM sodium phosphate, 250 mM sodium chloride, pH 7.0). A 200 μ L sample was filtered through a 0.2 μ m membrane (Millex GV, Millipore, France) and subjected to FPLC size-exclusion chromatography (SEC) on a Superdex-Peptide HR10/30 column (Pharmacia) equilibrated with buffer A. Detection wave-

length and flow were 280 nm and 0.5 mL·min⁻¹, respectively. The column was previously calibrated with staphylococcal nuclease, intestinal fatty acid-binding protein, aprotinin, insulin, and Ac-CAKYKELGYQG-NH₂. The extract fraction, ranging from 1.5–15 kDa, was collected and subjected to reverse-phase HPLC on a Delta Pack column (15 μ m, C-18, 300 Å, 7.8 \times 300 mm; Waters). The gradient was 2.0%·min⁻¹, between 0.07% (v/v) trifluoroacetic acid and 75% acetonitrile/0.05% trifluoroacetic acid (v/v/v). The absorbance was monitored at 215 and 278 nm, and the flow was set to 2.9 mL·min⁻¹. HPLC fractions, eluting between 47.7% and 51.0% acetonitrile (v/v), were collected and concentrated to 200 μ L (speed-vac; Savant Instrument, Inc. Holbrook, NY, USA). Disulfides in the collected fractions were reduced by adding concentrated or solid reagents to 8 M guanidinium chloride, 300 mM Tris/HCl, pH 8.5, 2.8 mM dithiothreitol, in a final volume of \approx 350 μ L, and by incubating the resulting solutions for 1 h at 37 °C in the dark. After reduction, 1 μ L of 4-vinylpyridine was added, and the incubation was continued for 1 h. The resulting cysteine-alkylated peptides were purified on a Vydac C-18 reverse-phase column (5 μ m, C-18, 300 Å, 2.1 \times 250 mm; Vydac Separation Group, Hesperia, CA, USA). The gradient was 0.5%·min⁻¹, between 0.07% trifluoroacetic acid (v/v) and 75% acetonitrile/0.05% trifluoroacetic acid (v/v/v). The flow was 0.2 mL·min⁻¹. UV detection was set to 215 and 254 nm. Two major peaks were subjected to sequencing by automated Edman degradation. This procedure yielded most of the PSKP-1 and PSKP-2 sequence. However, to assign the C-terminal residues, it was necessary to perform peptide mapping. Proteolysis was achieved by adding 0.15 μ g of V8 protease to 65 pmol of pyridylethylated peptides in 30 μ L of 100 mM ammonium bicarbonate, pH 7.8. After a 20 h incubation at 37 °C, products were separated by HPLC, as described above, and sequenced.

Expression and purification of recombinant proteins

PSKP-1 encoding DNA was custom synthesized and ligated into a cloning vector by Interactiva Inc. (Ulm, Germany). Codon usage was optimized for expression in *E. coli* [22]. The fragment encoding recombinant PSKP-1 was subcloned into pET-15b (Novagen) at *Nco*I and *Bam*HI sites. The resulting expression vector, pET-PSKP-1, was sequenced to confirm the reading frame and the identity of the insert.

For expression, *E. coli* BL21 (DE3) cells were transformed with pET-PSKP-1 and grown to saturation [overnight at 37 °C in LB (Luria-Bertani) broth containing 100 mg·mL⁻¹ ampicillin]. The saturated culture (2 mL) was used to inoculate 1 L of fresh broth, and growth was continued to reach an attenuation (*D*), at 600 nm, of \approx 1. Then, either 1 mM isopropyl thio- β -D-galactoside or 1% (w/v) lactose was added, and incubation continued for 3 h. Cells were harvested by centrifugation at 5000 g (10 min at 4 °C), and the resulting pellet was stored at -20 °C. As PSKP-1 was present in inclusion bodies, harvested cells (3–4 g) were suspended in 8 mL of lysis buffer (50 mM Tris/HCl, 100 mM NaCl, 1 mM EDTA, pH 8.0) and disrupted by sonication in an ice bath (in 4 mL fractions, five pulses of 30 s and 4 watts). Inclusion bodies were isolated by centrifugation (12 000 g, 10 min, 4 °C), and several

contaminants were removed by successive incubation/centrifugation cycles, as follows: (a) with 10 mM MgCl₂, 10 µg·mL⁻¹ DNase I in lysis buffer (30 min at 37 °C), (b) with 10 µg·mL⁻¹ DNase I in lysis buffer (30 min at 37 °C), (c) with 0.2 mg·mL⁻¹ lysozyme in lysis buffer (15 min at room temperature), (d) with 2 mg·mL⁻¹ sodium deoxycholate in lysis buffer (10 min at room temperature), (e) with 0.5% (v/v) Triton X-100 in lysis buffer (10 min at room temperature) and, finally, (f) with three incubation/centrifugation cycles in water. Cleaned inclusion bodies were solubilized at 37 °C in buffer B (20 mM sodium phosphate, 8 M urea, 2 mM glycine, 50 mM dithiothreitol, pH 7.5) and loaded onto an SP Sepharose Fast-Flow (Pharmacia Biotech) cationic exchange column (1.5 × 5.0 cm) equilibrated with buffer B. Elution was performed with a 200 mL linear gradient of 0–0.5 M NaCl in buffer B. Fractions were monitored by absorbance at 280 nm and SDS/PAGE. Fractions containing pure PSKP-1 were dialyzed, first overnight at 5 °C against 100 volumes of 20 mM sodium phosphate, 5.0 mM 2-mercaptoethanol, 0.5 mM cystamine, pH 7.5, and then exhaustively against distilled water. Finally, particulate matter was removed by centrifugation (24 000 *g*, 20 min, 4 °C) and the solution fast-frozen to –80 °C and lyophilized. The resulting product was stored at –20 °C.

Mutagenesis of recombinant PSKP-1

A PSKP-1 variant, PSKP-1^K (Fig. 2), with L, P, G and K at P₆, P₅, P₄ and P₁, respectively, was prepared by genetic engineering. DNA encoding PSKP-1^K was produced by site-specific PCR mutagenesis and a combination of overlapping fragments [23], using pET-PSKP-1 as the template and primers 5'-CTGCCAGGCTGCCCGAAAGATATT AACCCGGTGTGC-3' and 5'-CGGGCAGCCTGGCAGTTCATATTTATAGCATTTCGG-3' (the mutated codons are underlined). The PCR product was cloned into pET-15b, as described above. The resulting expression vector was termed pET-PSKP-1^K.

Inhibition of α-caseinolysis

Inhibition of α-caseinolysis [24] was performed as follows. Bovine trypsin (≈ 80 pmol) was preincubated for 20 min at 37 °C with a 10- or 100-fold molar excess of the inhibitor in 450 µL of 25 mM Tris/HCl, 100 mM sodium chloride, pH 7.4. Then, proteolysis was started by the addition of 50 µL of 10 mg·mL⁻¹ α-casein. At different time-points, 60 µL aliquots were withdrawn and the reaction was stopped by the addition of 60 µL of 1.8 M trichloroacetic acid. After incubation at 0 °C for 30 min, the precipitate was removed by centrifugation (12 000 *g*, 15 min, 4 °C) and the supernatant absorbance at 280 nm was measured. Controls (with the inhibitor or the protease omitted) were included. Assays for inhibitory activity towards chymotrypsin, *Staphylococcus aureus* strain V8 protease, and proteinase K were performed similarly, changing the assay buffer as appropriate.

Inhibition of Z-Arg-pNA trypsinolysis

Inhibition of trypsin activity towards Z-Arg-pNA was assessed using a Shimadzu UV 160A spectrophotometer

equipped with a thermostatic cell holder and a 50 µL quartz cell. Aliquots of 50 µL of enzyme solution (48 nM bovine trypsin, 100 mM Tris/HCl, 400 mM sodium chloride, 0.01% (w/v) NaN₃, pH 7.4) were preincubated with 45 µL of inhibitor solution (0–50 µM in water) for 5 min at 30 °C. Then, 5 µL of substrate, in dimethylformamide, was added to a final concentration of 2.5 mM, and formation of the product was monitored by absorbance at 405 nm (1–5 min at 30 °C). Three independent experiments were performed, in which each inhibitor concentration was assayed in duplicate. K_i^{app} , the apparent inhibition constant, was calculated as described previously [25], by fitting the following equation to the data:

$$\frac{v_i}{v_0} = \frac{1}{1 + \frac{[I]}{K_i^{app}}} \quad (1)$$

where v_i and v_0 are the initial reaction velocities in the presence and absence of inhibitor, respectively, and $[I]$ is the inhibitor concentration. The enzyme–inhibitor dissociation constant, K_i , was calculated as follows:

$$K_i = \frac{K_i^{app}}{1 + \frac{[S]}{K_m}} \quad (2)$$

where $[S]$ is the concentration of substrate and $K_m = 0.79 \pm 0.10$ mM (as determined previously by using a substrate concentration of 0.06–5.0 mM, in the absence of inhibitor, and by fitting the Michaelis–Menten equation to the data).

Prolyl endopeptidase inhibition assay

Prolyl endopeptidase activity from bovine blood serum [26] was measured using Z-Gly-Pro-2NNAp as the substrate [27]. Assay samples were prepared by mixing 20 µL of bovine blood serum with 1960 µL of 0–20 µM inhibitor in 20 mM sodium phosphate, 150 mM sodium chloride, pH 7.4. After 30 min at 37 °C, the reaction was started by the addition of 20 µL of 5 mM Z-Gly-Pro-2NNAp in methanol. The formation of naphthylamine was continuously monitored by fluorescence (4–6 min at 37 °C; excitation and emission were at 340 and 410 nm, respectively). Enzyme reaction controls, containing either no substrate or no bovine blood serum, were included. Negative controls for the inhibitory activity, in which either lysozyme or recombinant Δ9 exo small β-lactamase [28] substituted for the inhibitor, were used to correct for nonspecific effects on the fluorescence [29]. Moreover, because Δ9 exo small β-lactamase is purified from inclusion bodies and refolded by the same protocol as that used to obtain the PSKP-1 variants, the latter control served to check for *E. coli* contaminants that may have inhibitory effects on the reaction. Two independent experiments were performed, and the following equation was fitted to the data:

$$\frac{v_i}{v_0} = \frac{(1 - A)}{\left(1 + \frac{[I]}{IC_{50}}\right)} + A \quad (3)$$

where v_i is the reaction velocity for each inhibitor concentration, v_0 was calculated for each concentration of the inhibitor by nonlinear fit of the data from the above negative controls; $[I]$ is the concentration of the inhibitor, IC_{50} is the concentration of inhibitor that causes 50% inhibition; and A is the noninhibitable activity.

CD experiments

CD spectra were obtained at 20 °C on a Jasco J-810 spectropolarimeter (Jasco Corporation, Tokyo, Japan). The scan speed was 20 and 50 nm·min⁻¹ (near- and far-UV, respectively), with a 1 s response time, 0.2 nm data pitch, and 1 nm bandwidth. The CD buffer was 25 mM sodium phosphate, 100 mM sodium fluoride, pH 7.0. Near-UV measurements were carried out in a 1.0-cm cell containing 30 μM protein. In the far-UV analysis, cell path and protein concentration were 0.2 cm and 5 μM, respectively. Ten scans were averaged for each sample and the corresponding blanks subtracted.

Size and aggregation state

Analytical size-exclusion chromatography (SEC) was carried out at 22 °C with an FPLC Superose 12 10/30 column, equilibrated and eluted with 100 mM sodium phosphate, pH 7.0, and UV detection at 280 nm (Pharmacia). Apparent molecular weights were calculated from a calibration curve of standard molecules (thyroglobulin, bovine γ-globulin, chicken ovalbumin, equine myoglobin, vitamin B12, bovine trypsin and aprotinin); theoretical Stokes radii were calculated assuming a spherical shape [30]. Chemical cross-linking experiments were performed with 0–0.5% (v/v) glutaraldehyde (Fluka, Buchs, Switzerland) for 0–30 min at room temperature. The protein concentration was 10–50 μM in 10 mM sodium phosphate, 150 mM NaCl, pH 7.0. The reaction was terminated by adding SDS/PAGE sample buffer and the samples were subjected to SDS/PAGE.

Fluorescence spectra

Steady-state fluorescence was recorded at 20 °C on a K2 ISS instrument (ISS, Champaign, IL, USA). Protein solutions (7.7 μM) were prepared in 100 mM sodium phosphate, pH 7.0. Lamp intensity fluctuations were corrected by measuring the sample-to-reference ratio using a quantum counter in the reference channel. Excitation was set to 295 nm (8 nm bandwidth), and data were acquired at 1 nm intervals between 250 and 500 nm. Quantum yield (Q) was calculated, as described previously [31], using tryptophan as the standard with $Q = 0.14$ [32].

Antibacterial activity assays

Antibacterial activity was measured, as previously described [33], with minor modifications. Briefly, 10 mL of LB broth was inoculated with 100 μL of an overnight culture of *E. coli* (ATCC 11229) and incubated at 37 °C, with shaking, to mid-logarithmic phase. Bacteria were washed three times with 10 mL of 10 mM sodium phosphate, pH 7.4 and diluted to 50–125 colony-forming units per microliter in 10 mM sodium phosphate, pH 7.4, supplemented with 1%

(v/v) LB broth. Proteins and peptides (samples) were dissolved in the same buffer and 100 μL of each dilution was added to 100 μL of the bacterial suspension and incubated at 37 °C. Aliquots of each culture were withdrawn after 2.5 h of incubation, and the number of viable cells was estimated by plating serial dilutions and colony counting. Results were normalized to the zero sample concentration, and the following equation [34] was fit to the data:

$$y = \frac{1}{1 + \left(\frac{[S]}{EC_{50}}\right)^b} \quad (4)$$

where $[S]$ is the concentration of the sample, EC_{50} is the effective concentration that causes 50% of the effect, and b represents the cooperativity of the effect.

Hemagglutination

Hamster, mouse and human erythrocytes were isolated from blood anticoagulated with EDTA, and, after removal of plasma and buffy coat by mild centrifugation, washed three times with 10 mM sodium phosphate, 150 mM sodium chloride, 0.01% sodium azide, pH 7.4. Protein samples (0.3–80 μM) in 200 μL of 1% (v/v) erythrocyte suspension, were incubated for 1 h at 37 °C, and the assay was considered positive if agglutination was apparent to the naked eye.

Results

Protein isolation and sequence assignments

The acidic extract prepared from the skin of a single *P. sauvagii* specimen was subjected to SEC (Fig. 1A). The peptide fraction, corresponding to 1.5–15 kDa apparent mass, was further analyzed by reverse-phase HPLC (Fig. 1B). One of the resolved products, with prominent UV absorption and low hydrophobicity (retention times 32–34 min) was partially sequenced. Although the material was impure (data not shown), homology to protease inhibitors with a high cysteine content was evident. Therefore, the rest of the fraction was concentrated, reduced with dithiothreitol under denaturing conditions, treated with vinylpyridine, and rechromatographed (Fig. 1C). Pyridylethylated peptides were recognized by their characteristic absorbance at 254 nm. The full sequence of PSKP-1 (Fig. 1C, peak 5) was established by Edman degradation and mass analysis (Fig. 2A). Direct sequencing yielded amino acids 1–43. Residues 33–58 were identified by sequencing a fragment of PSKP-1 obtained by V8-protease treatment and peptide mapping (data not shown). The whole sequence of PSKP-1 was confirmed by mass analysis of the pyridylethylated protein, which yielded a molecular mass value of 7332.0 ± 0.7 Da (calculated molecular mass 7332.8 Da). The same sequencing strategy was applied to PSKP-2 (Fig. 1C, peak 6). Direct sequencing yielded amino acids 1–46; however, peptide mapping of V8-digested PSKP-2 was unsuccessful because of the scarcity of material. Nevertheless, based on mass analysis and homology to PSKP-1, a tentative full sequence of PSKP-2 is proposed (Fig. 2A). If residues 47–58 of

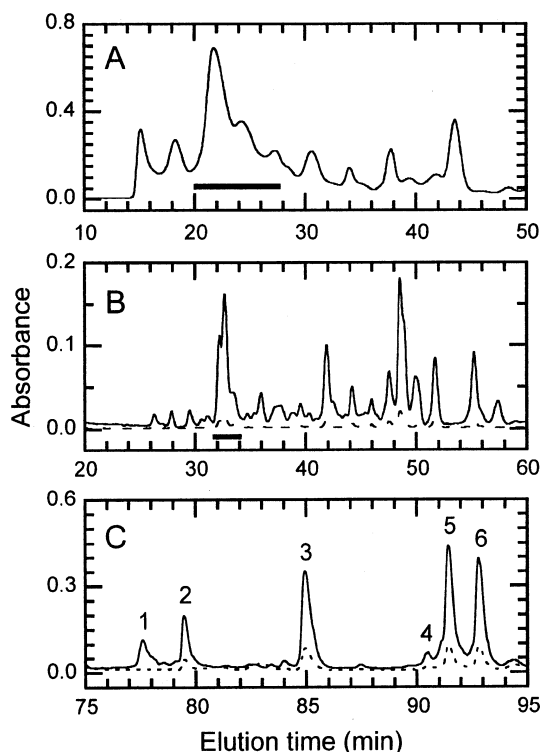


Fig. 1. Isolation of *Phyllomedusa sauvagii* Kazal protein 1 and 2 (PSKP-1 and PSKP-2, respectively) from a *P. sauvagii* skin extract. (A) FPLC-size exclusion chromatography. The bar indicates the fraction comprising 1.5–15 kDa peptides. The full line represents absorbance at 280 nm. (B) The above fraction was chromatographed on a semipreparative reverse-phase column. Solid and dashed lines represent the absorbance at 215 and 280 nm, respectively. (C) The fraction indicated in (B) was reduced with dithiothreitol under denaturing conditions, cysteine residues were blocked with 4-vinylpyridine, and modified peptides were separated on an analytical reverse-phase column. The solid line represents the absorbance at 215 nm. The signal at 254 nm is indicated by dashes. Fractions 5 and 6 were subsequently proven to contain pure pyridylethylated PSKP-1 and PSKP-2, respectively. Fractions 1–4 were retained for future studies.

PSKP-2 are assumed to be equal to those of PSKP-1, a calculated mass for the pyridylethylated protein is obtained, which is within 0.5 Da of the experimental value (7185.8 vs. 7185.3 Da).

Bioinformatic studies

According to standard amino acid pK_a in water, the theoretical pI of unfolded and fully reduced PSKP-1 is 9.8, whereas the pI value for PSKP-2 is 9.1. Although both proteins are highly basic, they differ by three charge units at physiological pH.

As only PSKP-1 was fully sequenced, further sequence comparisons were restricted to this variant. A search showed that PSKP-1 matched perfectly the consensus pattern for Kazal domains: C-x(7)-C-x(6)-Y-x(3)-C-x(2,3)-C (PROSITE PDOC00254), and therefore it is homologous to PSTI, acrosin inhibitor, ovomucoid, and to other extracellular matrix proteins that are not protease inhibitors but contain Kazal-like motifs. The closest relatives of PSKP-1 are serine

protease inhibitors, and a few examples are shown in Table 1. Besides the consensus Kazal residues, PSKP-1 exhibits Asn at position 31, a structurally important residue strongly conserved among serine protease inhibitors [35].

PSKP-1 differs from all reported Kazal serine protease inhibitors in having proline at both P_1 and P_2 . Six Kazal-like proteins were found in the Pfam protein families database [36], with two prolines in these positions, but none was a protease inhibitor and they departed from the canonical pattern by having extra residues between cysteines and, in some cases, also missing cysteines. Four were putative osteonectin fragments and products of the SPARC gene (Q9PU25, SPL1_RAT, SPL1_MOUSE, SPL1_HUMAN), the fifth was a hypothetical protein from *Homo sapiens* (Q8N4S1), and the sixth (Q9VSK1) was a putative protein from *Drosophila melanogaster*. In addition, the segment between the ultimate and penultimate cysteines has 10–18 residues in the inhibitors reported previously, whereas it is 21 residues long in PSKP-1 (Table 1). Interestingly, the latter segment is extremely basic in PSKP-1, having a net charge of +6 (the next larger charge found for this fragment in the data bank was +5.5 and corresponded to IAC2_BOVIN).

Expression, purification, and refolding

The synthetic gene encoding PSKP-1 (Fig. 2B) was over-expressed in *E. coli* to $\approx 10\%$ of total protein. SDS/PAGE analysis indicated that the recombinant protein accumulated in inclusion bodies. PSKP-1 was dissolved under strong denaturant and reducing conditions and then purified to homogeneity, taking advantage of its strongly basic properties. SDS/PAGE analysis of the purified product evidenced $> 95\%$ purity and an apparent molecular weight of 8000 (not shown). Pure unfolded and reduced recombinant PSKP-1 was refolded by dialysis against a disulfide-containing buffer with a yield of 13 mg of folded protein per litre of cell culture. Mass analysis indicated that post-translational removal of the initial Met did not take place to a significant extent (observed mass, 6828.3 ± 2.6 Da; predicted mass, 6827.2 Da), and the complete formation of disulfide bridges was confirmed by Ellman's reaction [21].

Optical studies

The far-UV CD spectrum of PSKP-1 is highly unusual (Fig. 3A), with a strong negative minimum at 209 nm, two distinct shoulders at 200 and 225 nm, and absence of the large positive maximum observed in nearly all folded proteins in the 185–195 nm region. However, the spectrum is similar to one reported by Watanabe *et al.* for the chicken ovomucoid first domain [37]. The near-UV CD spectrum (Fig. 3) shows fine structure on a negative envelope extending up to 320 nm. The broad negative band is probably caused by the high disulfide content.

PSKP-1 fluorescence emission is centered at 347 nm, which is typical of tryptophan in a hydrophobic environment. Moreover, the emission is poorly quenched by nearby groups or solvent molecules; the quantum yield is 0.21 for native PSKP-1, whereas the value for a fully exposed tryptophan is 0.14 (data not shown).

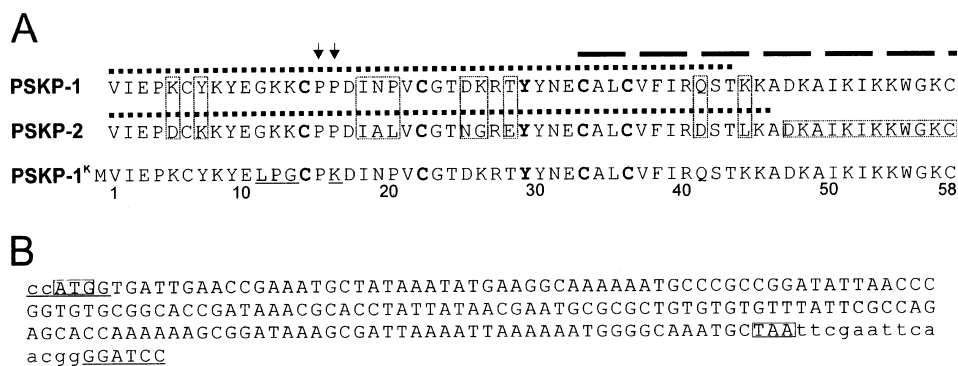


Fig. 2. *Phyllomedusa sauvagii* Kazal protein 1 and 2 (PSKP-1 and PSKP-2, respectively) sequences. (A) The dotted line indicates residues determined by N-terminal degradation from full-length pyridylethylated proteins. The dashed line shows sequence results obtained from an HPLC-isolated peptide after V8 protease digestion of pyridylethylated PSKP-1. Scarcity of material precluded sequencing of V8 peptides of PSKP-2. However, based on mass spectrometry (see the Results) and homology to PSKP-1, C-terminal residues were assigned tentatively, as shown in the horizontal box. Vertical boxes highlight differences between PSKP-1 and PSKP-2. Four cysteines and one tyrosine, conforming to the Kazal consensus motif (see the text), are represented in bold case. Right and left arrows indicate P₁ and P₂ active-site residues, respectively (Schechter & Berger notation) [53]. The residues underlined are those substituted in PSKP-1 by site-directed mutagenesis. (B) Synthetic DNA sequence used for *Escherichia coli* expression of recombinant PSKP-1. The encoding sequence is in upper case letters, with start and stop codons in boxes. Flanking restriction sites introduced for cloning purposes are underlined.

Table 1. Representative proteins homologous to *Phyllomedusa sauvagii* Kazal protein 1 (PSKP-1). After an initial search with BLAST [54], alignment to PSKP-1 was optimized manually. 1HPT and 2OVO are two examples of Kazal domains included in the Protein Data Bank. Conserved residues are underlined. Bold text shows consensus residues in the Kazal pattern. 2OVO, *Lophura nycthemera* ovomucoid third domain (PDB entry); IAC2, *Homo sapiens* acrosin-trypsin inhibitor II precursor, sp.|P20155|IAC2_HUMAN; 1HPT, *Homo sapiens* pancreatic secretory trypsin inhibitor variant 3 (PDB entry); IAC, *Macaca fascicularis*, acrosin-trypsin inhibitor II precursor, sp.|P34953|IAC_MACFA. X, any residue; B and Z represent the active site residues P₂ and P₁, respectively, in Schechter & Berger notation [53].

Protein	Sequence	Identity (%)
2OVO	AVSVD <u>C</u> SEYP KPACTMEYRP LCGSDNKTYG <u>NKCNFC</u> NAVVE S---NG-TL TLSHF <u>GKC</u>	28
IAC2	YRTPN <u>C</u> SQYR LPG <u>C</u> PRHFNP VCGSDMSTYA <u>NECTL</u> CMKIR E---GGHNI <u>KIIRNGPC</u>	43
IPK1 ^a	QREATC-TSE VSG <u>C</u> PKIYNP VCGTDGITYS <u>NECVL</u> CFEN- ---KKRQTPV <u>LIQKSGPC</u>	43
IPK1 ^b	GRDANC-NYE FPG <u>C</u> PRNLEP VCGTDGNTYN <u>NECLL</u> CMEN- ---KKRDVPI <u>RIQKDGPC</u>	45
1HPT	GREAK <u>C</u> YN-E LNG <u>C</u> TYEYRP VCGTDGDTYP <u>NECVL</u> CFENR ---KR-QTSI <u>LIQKSGPC</u>	45
IAC	YKTPF <u>C</u> ARYQ LPG <u>C</u> PRDFNP VCGTDMITYP <u>NECTL</u> CMKIR ES---GQNI <u>KILRRGPC</u>	48
PSKP-1	VIEPK <u>C</u> YKYE GKK <u>C</u> PPDINP VCGTDKRTY <u>NECAL</u> CVFIR QSTKKADKA <u>I KIKKWGKC</u>	100
	1 10 20 30 40 50 58	
Kazal pattern	----- <u>C</u> ----- <u>CBZ</u> XXXX <u>X</u> CXXXXXXXX <u>YX</u> XX <u>C</u> XX <u>C</u> ----- <u>C</u>	

^a *Sus scrofa*, pancreatic secretory trypsin inhibitor, sp.|P00998|IPK1_PIG. ^b *Monodelphis domestica*, pancreatic secretory trypsin inhibitor, sp.|P81635|IPK1_MONDO.

Hydrodynamic behavior and aggregation state

In SEC experiments, the Stokes radius of PSKP-1 was found to be 17.4 ± 0.2 Å. This value is larger and smaller than expected for a spherical molecule of 6.8 kDa (14.5 Å) and 13.6 kDa (18.7 Å), respectively [30]. To determine whether PSKP-1 was homodimeric in solution, chemical cross-linking experiments were performed. The results indicated that the protein is essentially monomeric in the 10–50 µM concentration range (data not shown). Therefore, the nonideal behavior in chromatography was attributed to departure from the spherical shape.

Biological activity

Given that PSKP-1 is homologous to Kazal-type serine protease inhibitors, it was tested in a caseinolytic assay

against trypsin, chymotrypsin, *S. aureus* strain V8 protease, and proteinase K. A typical experiment with trypsin is shown in Fig. 4. Whereas full inhibition is achieved by adding aprotinin at a 10-fold molar excess over the protease, PSKP-1 is inactive, even at a 100-fold molar excess.

Altering active-site specific contacts affects the strength of the inhibition by Kazal inhibitors [35]. Based on the sequences of acrosin inhibitor – a trypsin-like serine protease inhibitor – a variant of PSKP-1 was prepared with Leu, Pro and Gly at P₆, P₅ and P₄, respectively, and with Lys at P₁ (Fig. 2). The new variant, PSKP-1^K has a similar expression level and was purified in the same way as PSKP-1. As expected, PSKP-1^K showed significant inhibitory activity on trypsin (Fig. 4). To further characterize the binding of PSKP-1 and PSKP-1^K to trypsin, a specific assay was performed using Z-Arg-pNA as substrate (data not shown). Binding of PSKP-1 was very weak, with a K_i^{app} of

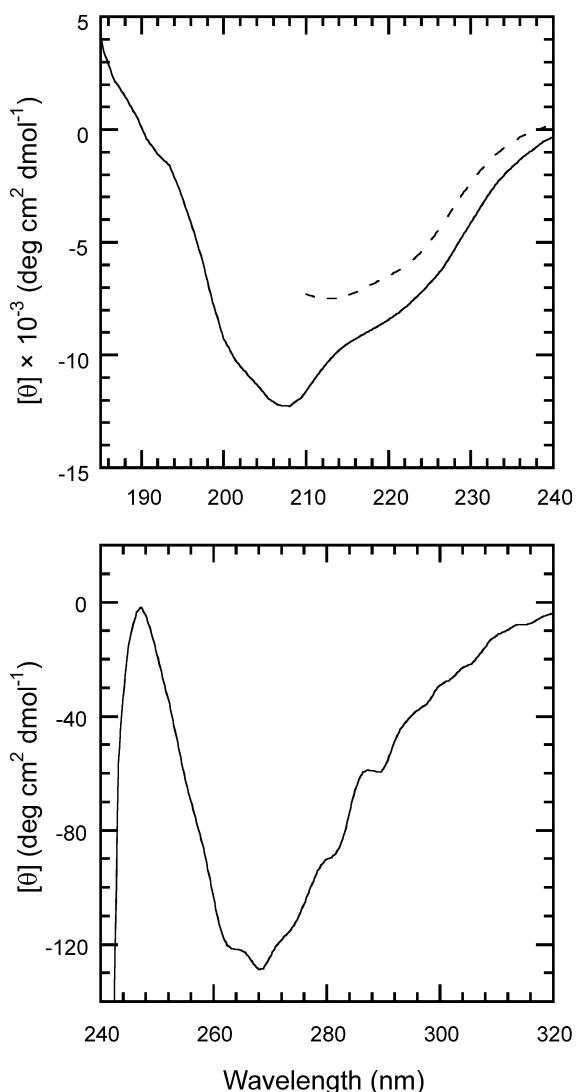


Fig. 3. Optical properties. (A) Far-UV CD spectrum of *Phyllomedusa sauvagii* Kazal protein 1 (PSKP-1) in 25 mM sodium phosphate, 100 mM sodium fluoride, pH 7.0 (solid line) and in 100 mM sodium phosphate, 3.8 M guanidinium chloride, pH 7.0 (dotted line). (B) Near-UV CD spectrum of PSKP-1 in 25 mM sodium phosphate, 100 mM sodium fluoride, pH 7.0.

> 0.5 mM and a K_i of > 0.1 mM. In contrast, the affinity of PSKP-1^K was very high, with a $K_i^{\text{app}} = 0.948 \pm 0.045 \mu\text{M}$ and $K_i = 228 \pm 11 \text{ nM}$ [Eqns (1) and (2) in the Materials and methods; results represent the mean \pm SD values of three independent experiments].

PSKP-1 and PSKP-1^K were also tested as inhibitors for prolyl endopeptidases. To achieve this, we used a crude preparation of bovine serum and Z-Gly-Pro-2NNap, as enzyme source and fluorescent specific substrate, respectively [27]. Two unrelated proteins, lysozyme and $\Delta 9$ exo small β -lactamase [28], were used as negative controls for the inhibitory activity. Because $\Delta 9$ exo small β -lactamase can be purified from inclusion bodies and refolded by the same protocol as that used to obtain the PSKP-1 variants, it served to check for *E. coli* contaminants that may have

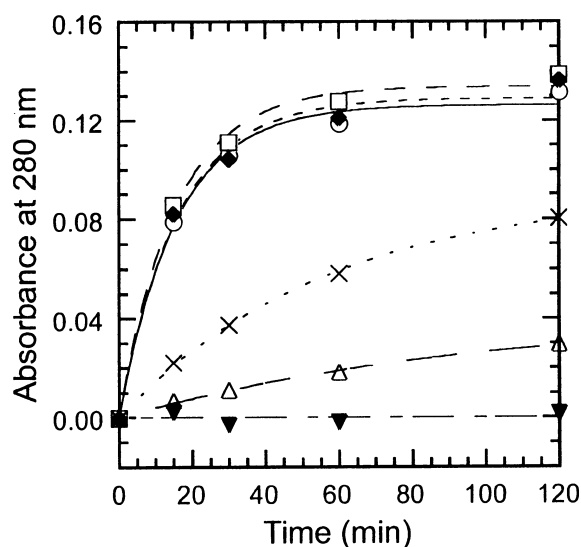


Fig. 4. Inhibition of α -casein proteolysis. A representative experiment, performed as described in the Materials and methods, is shown. Trypsin was incubated with a suspension of α -casein. After precipitation with trichloroacetic acid and centrifugation, proteolysis was estimated by measuring the absorbance of the supernatant at 280 nm. Circles represent hydrolysis by trypsin. Inverted triangles represent hydrolysis by trypsin pretreated with a 10-fold molar excess of aprotinin. Squares and diamonds show the effect of preincubation with 10- and 100-fold molar excess of *Phyllomedusa sauvagii* Kazal Protein 1 (PSKP-1). Crosses and normal triangles show the inhibitory effect of 10- and 100-fold molar excesses of PSKP-1^K (a PSKP-1 variant with L, P, G and K at positions P₆, P₅, P₄ and P₁, respectively).

inhibitory effects on the reaction. Both PSKP-1 and PSKP-1^K were found to be good inhibitors (Fig. 5). After the appropriate corrections for nonspecific effects of the control proteins on the fluorescence [29], the calculated IC_{50%} values for PSKP-1 and PSKP-1^K were 124 ± 56 and $131 \pm 26 \text{ nM}$, respectively. Interestingly, 24–32% residual activity remained that could not be inhibited by the assayed proteins, and was probably caused by the existence of more than one type of prolyl endopeptidase in the serum [26,29,38].

Other possible biological activities were also tested. Neither PSKP-1 nor PSKP-1^K showed hemolytic activity. However, at a micromolar concentration, both hemagglutinate hamster, mouse, and human erythrocytes. Hemagglutination by PSKP-1 and PSKP-1^K was inhibited by EDTA and heparin.

Certain basic proteins have ancillary antibacterial activity. Some examples are aprotinin, SLPI, and CAP18 [39,40]. All seem to interact with bacterial membranes, although the molecular basis of this action is not well understood. To test whether PSKP-1 and PSKP-1^K pertain to this group of proteins, they were assayed against *E. coli* (data not shown). Aprotinin and PSKP-1^K have similar potency in the assay, with an EC₅₀ of 0.9 and 1.4 μM , respectively. PSKP-1 is slightly less potent, with an EC₅₀ of 3.0 μM . Four to six assays were performed with each sample, the interassay error was less than 30%, and the difference between PSKP-1 and PSKP-1^K was significant ($P < 0.002$).

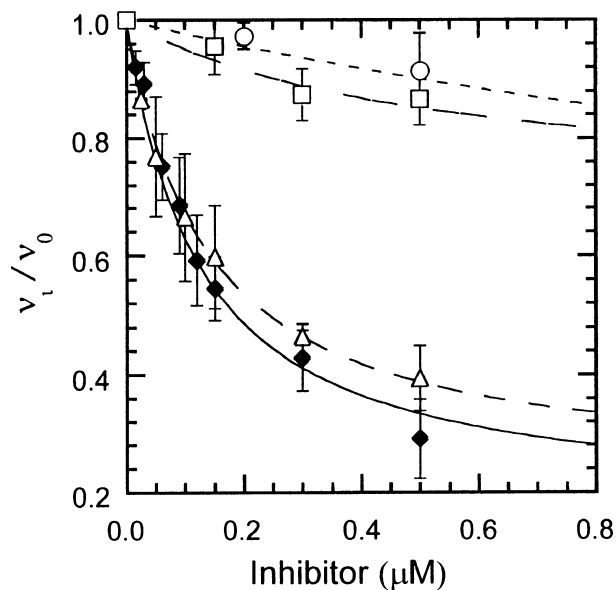


Fig. 5. Prolyl endopeptidase inhibition assay. Samples, inhibitors and control proteins were preincubated with an enzymatically active bovine serum preparation [26], and the reaction was started by the addition of the prolyl endopeptidase specific substrate, Z-Gly-Pro-2NNap (*N*-benzyloxycarbonyl-glycyl-prolyl-2-naphthylamide) [27] (see the Materials and methods). Relative activity is shown as a function of the concentration of each sample. Two independent experiments were carried out, and the error bars represent standard deviations. Samples were *Phyllomedusa sauvagii* Kazal protein 1 (PSKP-1) (◆), PSKP-1^K (a PSKP-1 variant with L, P, G and K at positions P₆, P₅, P₄, and P₁, respectively) (△), lysozyme (□), and Δ9 exo small β-lactamase (○).

In connection with the bactericidal activity of PSKP-1 and PSKP-1^K, a qualitative test was performed using *E. coli* ATCC 11229. This strain exhibits high mobility in low-salt liquid media, a feature that can be observed by optical microscopy. At micromolar concentrations, both proteins greatly reduce bacterial mobility and induce cell agglutination (data not shown).

Discussion

In this work, we report on PSKP-1 and PSKP-2, two variants of a new protein isolated from the skin of the anuran, *P. sauvagii*, whose sequence indicates membership of the Kazal family. Most members of this family are small protein inhibitors of serine proteases and have a characteristic pattern of disulfide bridges [41]. There exist, however, Kazal-like domains in larger multidomain extracellular matrix proteins which are not protease inhibitors [42]. From sequence homology analysis, PSKP-1 and PSKP-2 clearly pertain to the serine protease inhibitor type of Kazal proteins. In particular, PSKP-1 is 48% identical to the inhibitor of acrosin – the major protease of mammalian spermatozoa – from the crab-eating monkey, *Macaca fascicularis* (Table 1).

Whereas many Kazal inhibitors have proline at P₂, only two were reported to have proline at P₁ [43,44]. PSKP-1 and PSKP-2 are unique in having proline residues at both P₁ and P₂. Our results indicated that PSKP-1 has no effect on the

activity of trypsin, chymotrypsin, V8-protease, or proteinase K. This was expected because proline at P₁ should not fit well into the S₁ pocket of these proteases. Nevertheless, PSKP-1 can be rendered active against trypsin by replacing its P₄, P₅, and P₆ residues with the corresponding residues of acrosin inhibitor and proline at P₁ with lysine (Fig. 2). Thus, not only is the sequence of PSKP-1 that of a serine protease inhibitor, but also its 3D structure is capable of harboring inhibitory activity.

The finding of proline at P₁ and P₂ in PSKP-1, led us to consider the possibility of having isolated an inhibitor of prolyl oligopeptidases [27,45–47]. The X-ray structure of porcine prolyl oligopeptidase complexed with the synthetic specific inhibitor, Z-Pro-prolinal, reveals that the two proline side-chains fit snugly into the corresponding S₁ and S₂ crevices [48]. Although these serine proteases are not inhibited by aprotinin, soybean trypsin inhibitor or chicken ovomucoid [49], the purification of endogenous peptidic inhibitors, ranging from 6.5–8 kDa, have been described [50–52]. To the best of our knowledge, structural information regarding these inhibitors is lacking.

In blood serum, two different serine proteases with prolyl oligopeptidase activity have been reported. They have similar molecular weight, substrate specificity, temperature sensitivity, and pH profile, but differ in susceptibility to Z-Pro-prolinal and in the ability to hydrolyze certain natural peptides [26,29]. We show, in this work, that PSKP-1, at submicromolar concentrations, has inhibitory activity towards at least one of these enzymes. Although the serum proteases tested in the assay are unlikely to be the natural targets of PSKP-1, they are representative of its class, and thus the reported activity may have biological significance.

Interestingly enough, the inhibitory power of PSKP-1^K is as strong as that of PSKP-1. Assuming that PSKP-1 and PSKP-1^K act by a standard mechanism and have canonical binding loops [41], proline should be better than lysine at the P₁ position, for inhibitors tend to have residues at the scissile bond that match the specificity of the cognate protease. However, mutagenesis and crystallographic studies showed that changes at P₁ sometimes lead to counterintuitive results. A striking example of this is a BPTI mutant with a Leu → Lys change at P₁, which acts as a good inhibitor of chymotrypsin. In fact, for the chymotrypsin–BPTI interaction, lysine is a better P₁ residue than valine, isoleucine, or alanine [41]. X-ray analysis showed that, in this case of lysine, the side-chain bends out of the S₁ pocket and forms two new hydrogen bonds that stabilize the interaction [41]. To explain the similarity in IC₅₀ for PSKP-1 and PSKP-1^K, two further aspects must be considered: first, as the proteases assayed are not the natural target of PSKP-1, the interaction reported herein might be suboptimal; and, second, the three additional changes at the active site of PSKP-1^K may compensate for the loss of strength in the interaction caused by the change at P₁.

In summary, we describe PSKP-1, a novel Kazal protein that acts *in vitro* as a prolyl endopeptidase inhibitor. Whether the biological role of PSKP-1 is to inhibit a yet-unidentified prolyl oligopeptidase resident in the amphibian skin or released from an external pathogen remains to be seen. Concomitantly, or alternatively, PSKP-1, as other small basic proteins, might act in the skin of *P. sauvagii* as a membrane-perturbing compound with antimicrobial

properties. Our work provides structural information for the new protein and a means of producing it in large quantities, enabling a wide search for its natural targets.

Acknowledgements

This work was supported by grants from Agencia Nacional de Promoción Científica y Técnica and Universidad Nacional de Quilmes, Argentina.

References

- Roseghini, M., Falconieri Erspamer, G., Severini, C. & Simmaco, M. (1989) Biogenic amines and active peptides in extracts of the skin of thirty-two European amphibian species. *Comp. Biochem. Physiol. C* **94**, 455–460.
- Flier, J., Edwards, M.W., Daly, J.W. & Myers, C.W. (1980) Widespread occurrence in frogs and toads of skin compounds interacting with the ouabain site of Na⁺, K⁺-ATPase. *Science* **208**, 503–505.
- Daly, J.W. (1995) The chemistry of poisons in amphibian skin. *Proc. Natl Acad. Sci. USA* **92**, 9–13.
- Clarke, B.T. (1997) The natural history of amphibian skin secretions, their normal functioning and potential medical applications. *Biol. Rev. Camb. Philos. Soc.* **72**, 365–379.
- Barra, D. & Simmaco, M. (1995) Amphibian skin: a promising resource for antimicrobial peptides. *Trends Biotechnol.* **13**, 205–209.
- Bevins, C.L. & Zasloff, M. (1990) Peptides from frog skin. *Annu. Rev. Biochem.* **59**, 395–414.
- Kikuyama, S., Yamamoto, K., Iwata, T. & Toyoda, F. (2002) Peptide and protein pheromones in amphibians. *Comp. Biochem. Physiol. B Biochem. Mol. Biol.* **132**, 69–74.
- Wegener, K.L., Brinkworth, C.S., Bowie, J.H., Wallace, J.C. & Tyler, M.J. (2001) Bioactive dahlein peptides from the skin secretions of the Australian aquatic frog *Litoria dahlii*: sequence determination by electrospray mass spectrometry. *Rapid Commun. Mass Spectrom.* **15**, 1726–1734.
- Erspamer, V., Falconieri Erspamer, G. & Cei, J.M. (1986) Active peptides in the skins of two hundred and thirty American amphibian species. *Comp. Biochem. Physiol. C* **85**, 125–137.
- Erspamer, V., Melchiorri, P., Falconieri Erspamer, G., Montecucchi, P.C. & de Castiglione, R. (1985) Phyllomedusa skin: a huge factory and store house of a variety of active peptides. *Peptides* **6** (Suppl. 3), 7–12.
- Mor, A., Amiche, M. & Nicolas, P. (1994) Structure, synthesis, and activity of dermaseptin b, a novel vertebrate defensive peptide from frog skin: relationship with adenoregulin. *Biochemistry* **33**, 6642–6650.
- Mor, A., Delfour, A., Sagan, S., Amiche, M., Pradelles, P., Rossier, J. & Nicolas, P. (1989) Isolation of dermenkephalin from amphibian skin, a high affinity delta selective opioid heptapeptide containing a D amino acid residue. *FEBS Lett.* **255**, 269–274.
- Rosengren, K.J., Daly, N.L., Scanlon, M.J. & Craik, D.J. (2001) Solution structure of BSTI: a new trypsin inhibitor from skin secretions of *Bombina bombina*. *Biochemistry* **40**, 4601–4609.
- Mignogna, G., Pascarella, S., Wechselberger, C., Hinterleitner, C., Mollay, C., Amiconi, G., Barra, D. & Kreil, G. (1996) BSTI, a trypsin inhibitor from skin secretions of *Bombina bombina* related to protease inhibitors of nematodes. *Protein Sci.* **5**, 357–362.
- Lai, R., Liu, H., Lee, W.H. & Zhang, Y. (2002) Identification and cloning of a trypsin inhibitor from skin secretions of Chinese red belly toad *Bombina maxima*. *Comp. Biochem. Physiol. B Biochem. Mol. Biol.* **131**, 47–53.
- Conlon, J.M. & Kim, J.B. (2000) A protease inhibitor of the Kunitz family from skin secretions of the tomato frog, *Dyscophus guineti* (Microhylidae). *Biochem. Biophys. Res. Commun.* **279**, 961–964.
- Ali, M.F., Lips, K.R., Knoop, F.C., Fritsch, B., Miller, C. & Conlon, J.M. (2002) Antimicrobial peptides and protease inhibitors in the skin secretions of the crawfish frog, *Rana areolata*. *Biochim. Biophys. Acta* **1601**, 55–63.
- Pellegrini, A., Thomas, U., Bramaz, N., Klausner, S., Hunziker, P. & von Fellenberg, R. (1996) Identification and isolation of the bactericidal domains in the proteinase inhibitor aprotinin. *Biochem. Biophys. Res. Commun.* **222**, 559–565.
- Ibrahim, H.R., Thomas, U. & Pellegrini, A. (2001) A helix loop helix peptide at the upper lip of the active site cleft of lysozyme confers potent antimicrobial activity with membrane permeabilization action. *J. Biol. Chem.* **276**, 43767–43774.
- Schägger, H. & von Jagow, G. (1987) Tricine-sodium dodecyl sulfate-polyacrylamide gel electrophoresis for the separation of proteins in the range from 1 to 100 kDa. *Anal. Biochem.* **166**, 368–379.
- Ellman, G. & Lysko, H. (1979) A precise method for the determination of whole blood and plasma. *Anal. Biochem.* **93**, 98–102.
- Nakamura, Y., Gojobori, T. & Ikemura, T. (2000) Codon usage tabulated from international DNA sequence databases: status for the year 2000. *Nucleic Acids Res.* **28**, 292.
- Higuchi, R. (1989) Using PCR to engineer DNA in PCR technology. In *Principles and applications for DNA amplification* (Erich, H.A., ed.), pp. 61–70. Stockton Press, New York.
- Laskowski, M. (1955) Trypsinogen and trypsin. *Methods Enzymol.* **2**, 26–36.
- Bieth, J.G. (1995) Theoretical and practical aspects of proteinase inhibition kinetics. *Methods Enzymol.* **248**, 59–84.
- Birney, Y.A. & O'Connor, B.F. (2001) Purification and characterization of a Z-Pro-proline-insensitive Z-Gly-Pro-7-amino-4-methyl coumarin-hydrolyzing peptidase from bovine serum – a new proline-specific peptidase. *Protein Expr. Purif.* **22**, 286–298.
- Yoshimoto, T., Ogita, K., Walter, R., Koida, M. & Tsuru, D. (1979) Post-proline cleaving enzyme. Synthesis of a new fluorogenic substrate and distribution of the endopeptidase in rat tissues and body fluids of man. *Biochim. Biophys. Acta* **569**, 184–192.
- Santos, J., Gebhard, L.G., Risso, V.A., Ferreyra, R.G., Rossi, J.P. & Ermacora, M.R. (2004) Folding of an abridged beta-lactamase. *Biochemistry* **43**, 1715–1723.
- Cunningham, D.F. & O'Connor, B. (1998) A study of prolyl endopeptidase in bovine serum and its relevance to the tissue enzyme. *Int. J. Biochem. Cell Biol.* **30**, 99–114.
- Uversky, V.N. (1993) Use of fast protein size-exclusion liquid chromatography to study the unfolding of proteins which denature through the molten globule. *Biochemistry* **32**, 13288–13298.
- Parker, C.A. & Rees, W.T. (1960) Correction of fluorescence spectra and measurement of fluorescence quantum efficiency. *Analyst* **85**, 587–600.
- Chen, R.F. (1967) Fluorescence quantum yield of tryptophan and tyrosine. *Anal. Lett.* **1**, 35–42.
- Hiemstra, P.S., Maassen, R.J., Stolk, J., Heinzl-Wieland, R., Steffens, G.J. & Dijkman, J.H. (1996) Antibacterial activity of antileukoprotease. *Infect. Immun.* **64**, 4520–4524.
- Neubig, R.R., Spedding, M., Kenakin, T. & Christopoulos, A. (2003) International Union of Pharmacology Committee on Receptor Nomenclature and Drug Classification. XXXVIII. Update on Terms and Symbols in Quantitative Pharmacology. *Pharmacol. Rev.* **55**, 597–606.
- Lu, S.M., Lu, W., Qasim, M.A., Anderson, S., Apostol, I., Ardelt, W., Bigler, T., Chiang, Y.W., Cook, J., James, M.N. *et al.*

- (2001) Predicting the reactivity of proteins from their sequence alone: Kazal family of protein inhibitors of serine proteinases. *Proc. Natl Acad. Sci. USA* **98**, 1410–1415.
36. Bateman, A., Birney, E., Durbin, R., Eddy, S.R., Howe, K.L. & Sonnhammer, E.L. (2000) The Pfam protein families database. *Nucleic Acids Res.* **28**, 263–266.
37. Watanabe, K., Matsuda, T. & Sato, Y. (1981) The secondary structure of ovomucoid and its domains as studied by circular dichroism. *Biochim. Biophys. Acta* **667**, 242–250.
38. Cunningham, D.F. & O'Connor, B. (1997) Identification and initial characterisation of a N-benzyloxycarbonyl-prolyl-proline (Z-Pro-proline)-insensitive 7-(N-benzyloxycarbonyl-glycyl-prolyl-amido)-4-methylcoumarin (Z-Gly-Pro-NH-Mec)-hydrolysing peptidase in bovine serum. *Eur. J. Biochem.* **244**, 900–903.
39. Cole, A.M., Liao, H.I., Stuchlik, O., Tilan, J., Pohl, J. & Ganz, T. (2002) Cationic polypeptides are required for antibacterial activity of human airway fluid. *J. Immunol.* **169**, 6985–6991.
40. Zarembek, K.A., Katz, S.S., Tack, B.F., Doukhan, L., Weiss, J. & Elsbach, P. (2002) Host defense functions of proteolytically processed and parent (unprocessed) cathelicidins of rabbit granulocytes. *Infect. Immun.* **70**, 569–576.
41. Laskowski, M. & Qasim, M.A. (2000) What can the structures of enzyme-inhibitor complexes tell us about the structures of enzyme substrate complexes? *Biochim. Biophys. Acta* **1477**, 324–337.
42. Hohenester, E., Maurer, P. & Timpl, R. (1997) Crystal structure of a pair of follistatin-like and EF-hand calcium-binding domains in BM-40. *EMBO J.* **16**, 3778–3786.
43. Laskowski, M. Jr, Kato, I., Ardelt, W., Cook, J., Denton, A., Empie, M.W., Kohr, W.J., Park, S.J., Parks, K., Schatzley, B.L., *et al.* (1987) Ovomuroid third domains from 100 avian species: isolation, sequences, and hypervariability of enzyme inhibitor contact residues. *Biochemistry* **26**, 202–221.
44. Apostol, I., Giletto, A., Komiyama, T., Zhang, W. & Laskowski, M. Jr (1993) Amino acid sequences of ovomucoid third domains from 27 additional species of birds. *J. Protein Chem.* **12**, 419–433.
45. Yoshimoto, T., Walter, R. & Tsuru, D. (1980) Proline-specific endopeptidase from *Flavobacterium*. Purification and properties. *J. Biol. Chem.* **255**, 4786–4792.
46. Cunningham, D.F. & O'Connor, B. (1997) Proline specific peptidases. *Biochim. Biophys. Acta* **1343**, 160–186.
47. Grellier, P., Vendeville, S., Joyeau, R., Bastos, I.M., Drobecq, H., Frappier, F., Teixeira, A.R., Schrevel, J., Davioud-Charvet, E., Sergheraert, C. & Santana, J.M. (2001) *Trypanosoma cruzi* prolyl oligopeptidase Tc80 is involved in nonphagocytic mammalian cell invasion by trypanomastigotes. *J. Biol. Chem.* **276**, 47078–47086.
48. Fulop, V., Bocskei, Z. & Polgar, L. (1998) Prolyl oligopeptidase: an unusual beta propeller domain regulates proteolysis. *Cell* **94**, 161–170.
49. Walter, R., Simmons, W.H. & Yoshimoto, T. (1980) Proline specific endo- and exopeptidases. *Mol. Cell. Biochem.* **30**, 111–127.
50. Yamakawa, N., Shimeno, H., Soeda, S. & Nagamatsu, A. (1994) Regulation of prolyl oligopeptidase activity in regenerating rat liver. *Biochim. Biophys. Acta* **1199**, 279–284.
51. Yokosawa, H., Miyata, M., Sawada, H. & Ishii, S. (1983) Isolation and characterization of a post proline cleaving enzyme and its inhibitor from sperm of the ascidian, *Halocynthia roretzi*. *J. Biochem. (Tokyo)* **94**, 1067–1076.
52. Yoshimoto, T., Tsukumo, K., Takatsuka, N. & Tsuru, D. (1982) An inhibitor for post-proline cleaving enzyme; distribution and partial purification from porcine pancreas. *J. Pharmacobiodyn.* **5**, 734–740.
53. Schechter, I. & Berger, A. (1967) On the size of the active site in proteases. I. Papain. *Biochem. Biophys. Res. Commun.* **27**, 157–162.
54. Altschul, S. & Koonin, E. (1998) Iterated profile searches with PSI-BLAST; a tool for discovery in protein databases. *Trends Biochem. Sci.* **23**, 444–447.